Applied Catalysis B: Environmental 127 (2012) 18–27

Contents lists available at SciVerse ScienceDirect

Applied Catalysis B: Environmental

journal homepage: www.elsevier.com/locate/apcatb

Electrochemical promotion of methane oxidation on impregnated and sputtered Pd catalyst-electrodes deposited on YSZ

F. Matei[a], D. Ciuparu[a], C. Jiménez-Borja[b], F. Dorado[b], J.L. Valverde[b], S. Brosda[c,*]

[a] Department of Petroleum Processing Engineering and Environmental Protection, Petroleum - Gas University of Ploiesti, 39 Bucuresti Bd, 100680 Ploiesti, Romania
[b] Department of Chemical Engineering (UCLM), Avda. Camilo José Cela 12, ES-13071 Ciudad Real, Spain
[c] Department of Chemical Engineering, University of Patras, Caratheodory St1, GR-26504 Patras, Greece

ARTICLE INFO

Article history:
Received 14 June 2012
Received in revised form 27 July 2012
Accepted 31 July 2012
Available online 10 August 2012

Keywords:
Methane oxidation
Electrochemical promotion
Pd catalyst-electrode
Wet impregnation
Sputtered catalyst-electrodes

ABSTRACT

The microstructure and electrochemical promotion of thin Pd catalyst-electrodes deposited on yttria-stabilized zirconia (YSZ) prepared either by sputter-deposition or wet impregnation has been studied for the complete oxidation of methane using XRD, XPS and steady state catalytic measurements in conjunction to electrochemical studies at temperatures 350–460 °C under various CH_4 to O_2 ratios. As prepared sputtered catalyst electrodes, which consist mainly of a Pd metal phase are able to electrochemically promote the CH_4 oxidation, while impregnated films, which mainly consist of a PdO phase, can be electropromoted only after in situ reduction. On both types of catalyst-electrodes the reaction exhibits electrophobic behavior under all experimental conditions of this study, i.e. the rate increases moderately with anodic polarization. For sputtered samples, negative current application causes a decrease of the catalytic rate which remains lower than the initial open circuit rate after current interruption. This is a new type of permanent electrochemical promotion and a poisoning index, β, is introduced to quantify the magnitude of this effect.

1. Introduction

Palladium-based catalysts are widely accepted to be the most effective ones for the complete oxidation of methane [1–5]. Recent research has been focused on the nature of the active PdO_x/Pd species [6–12], since it has been shown that the catalytic activity is strongly affected by the chemical states of palladium. For a given and well defined Pd catalyst/support system, the catalytic activity is governed by the reaction conditions, i.e. temperature, methane/oxygen ratio and presence or absence of water. Furthermore, methane combustion rates differ under conditions when the catalyst is cycled in temperature [1]. The degree of hysteresis has been assigned to the reduction of PdO to Pd (and its reoxidation) accompanied by morphological changes of the catalyst.

1.1. Deep methane combustion on Pd–PdO deposited on YSZ

It is commonly accepted that at low temperatures the active phase is crystalline PdO, which may exist in more than one form, depending on oxidized particles size and on the kind of support [13–17]. At high temperatures (>800 °C), metallic Pd can also be active for methane oxidation. The nucleation and growth of PdO is favored over ZrO_2-based and CeO_2-promoted materials due to strong metal support interaction, i.e. the effective transfer of lattice oxygen to the catalyst [18,19].

The rate of oxidation of pre-reduced palladium catalysts is sensitive to previous thermal treatment and thus the catalytic activity [6]. The exact morphology of individual particles of oxidized palladium is strongly dependent on treatment temperature, time of exposure and gas composition, i.e. on the use of hydrogen or hydrocarbons for reduction [20–22].

1.2. Electrochemical properties of Pd/PdO catalyst electrodes deposited on oxides

Pd catalyst-electrodes deposited on oxide ion conducting supports, i.e. YSZ or Gadolinia oxide-doped CeO_2 (GDC) are used in semiconductor gas sensors for the selective and sensitive monitoring of air pollutants such as CO, H_2 or hydrocarbon [23–25] and for light hydrocarbon combustion in solid electrolyte fuel cells [26–28]. In both cases it is of interest to predict the stability of the Pd–PdO phase system at the gas exposed part of the catalyst-electrode as well as of the three phase boundary (tpb), the interface between support, catalytic film and gas phase. Studies carried out by Mizsei et al. [29] focused on the surface of the catalytic film. They studied the structure and resistivity of ultra-thin sputtered Au, Pd and Pt deposited on SiO_2 or SnO_2 during

* Corresponding author. Tel.: +30 2610 997576; fax: +30 2610 997269.
E-mail address: brosda@chemeng.upatras.gr (S. Brosda).

0926-3373/$ – see front matter © 2012 Elsevier B.V. All rights reserved.
http://dx.doi.org/10.1016/j.apcatb.2012.07.035

heat treatment. Sheet resistance measurements on 5 nm thin Pd sputtered films revealed a sudden resistance increase by many orders of magnitude at relatively low temperatures (470–500 °C) during heating. Current–voltage characteristic have been studied over Pd/YSZ electrodes in absence and presence of fuels, e.g. H_2, CH_4, or C_2H_4. Work by de Bruin et al. [30,31], Kaneko et al. [32] focused on electrochemical impedance spectroscopy (EIS) where the AC impedance response of the Pd/YSZ electrode is investigated in dependence on temperature and oxygen partial pressure. They found that bulk and electrode resistance are changing abruptly at the decomposition pressure of the PdO phase to Pd^0, or vice versa. The obtained resistance data show a hysteresis for both, their temperature dependence at constant P_{O_2} and oxygen partial pressure dependence at constant temperature. Kalimeri et al. [33] focused on steady-state polarization measurements on the O_2, Pd/YSZ interface and examined the charge transfer reaction mechanism. In presence of fuels only a few electrochemical studies on the Pd/YSZ interface have been carried out in conjunction to electrochemical promotion studies for the oxidation of ethylene [34] and methane [35–37].

1.3. Electrochemical promotion of methane oxidation on noble metals

Electrochemical promotion (EPOC) or non-Faradaic electrochemical modification of catalytic activity (NEMCA effect) is used to electrochemically promote metal or non-metal catalyst films for a variety of reactions including the deep oxidation of light hydrocarbons [38–42]. In an electrochemical promotion experiment the catalyst film is in contact to an ion-conducting support and serves simultaneously as a catalytic active phase and as a working electrode. The promoter species is electrochemically generated at the tpb, i.e. at the interphase of the support, the catalyst and the gas phase, by the application of a potential between the catalyst film and a counter electrode. Studies based on surface science and electrochemical techniques have shown that under polarization the promoting ionic species migrates in an electrochemically controlled manner from the tpb to the gas exposed surface. This electrochemically controlled promoting ion spillover can lead to a significant enhancement in catalytic rate which is higher than anticipated from the rate of supply of the promoting species.

Two parameters, the rate enhancement ratio, ρ, and the Faradaic efficiency, Λ, are commonly used to define the effect of potential on the catalytic activity.

The rate enhancement ratio, ρ, is defined as [42]:

$$\rho = \frac{r}{r_o} \quad (1)$$

where r_o is the catalytic rate at open circuit and r the catalytic rate under polarization and the Faradaic efficiency, Λ, is defined as [42]:

$$\Lambda = \frac{r - r_o}{I/nF} \quad (2)$$

where I is the applied current, F is Faradays constant, and $I/2F$ equals the rate of promoter supply to the catalyst. Since in this study Y_2O_3-stabilized-ZrO_2 (YSZ) is used as an excellent O^{2-} conducting support, n equals 2. A reaction exhibits electrochemical promotion when $|\Lambda| > 1$, while electrocatalysis is limited to $|\Lambda| \leq 1$ [42].

The electrochemically promoted deep oxidation of methane has been previously studied for the following three noble metal catalyst-electrodes: on Pt/YSZ [43], on Rh/YSZ [44,45] and on Pd/YSZ [36,37,46–50].

Table 1 summarizes the main results for the Pd/YSZ system. The catalytic activity of Pd catalysts prepared by organometallic paste deposition on YSZ is significantly electropromoted with a rate increase of up to 70–90 times under anodic polarization [36,37]. This study has been focused only on fuel rich conditions, while recent studies have been carried out exclusively under fuel lean conditions [46–50]. Only at relatively high temperatures of 470–600 °C Roche et al. [46] and Jiménez-Borja et al. [48] have noticed a rate enhancement on sputtered Pd films and on impregnated Pd catalysts, respectively, by applying a positive potential to the working electrode. The observed rate enhancement ratios are relatively low, i.e. 3 and 2.6 respectively. In the most recent studies by Jiménez-Borja et al. [49,50] the deep methane oxidation in excess of oxygen has been successfully electropromoted at low temperatures, 350 °C, after exposing the sample to a reactive ethylene/oxygen mixture or upon co-feeding small concentrations of C_2H_4 to the methane–oxygen inlet.

Table 1
Summary of electrochemical promotion studies on Pd based catalyst–electrodes in the deep methane oxidation reaction.

Catalyst	T (°C)	Λ_{max}	ρ_{max}	Ratio P_{O_2}/P_{CH_4}	References
Pd paste	>380	2×10^3	90	$P_{O_2} < P_{CH_4}$	[36,37]
Pd sputtered	>500	2.6×10^2	2.5	$P_{O_2} > P_{CH_4}$	[47]
Pd wet impregnated	>550	40–170	3	$P_{O_2} > P_{CH_4}$	[49]
	>320	63–66	1.2–1.7	$P_{O_2} > P_{CH_4}$	[51]

The aim of the present work was to investigate and compare Pd catalyst electrodes prepared via sputter-deposition and via wet impregnation method and to clarify the influence of the Pd^0/PdO redox couple on the catalytic oxidation of methane. Catalytic studies were combined with in situ resistance measurements and with the characterization of as prepared and spent catalysts to relate this influence to the ability to electrochemically promote CH_4 combustion over Pd/YSZ.

2. Experimental

2.1. Catalyst preparation

A disk of 8 mol% Y_2O_3-stabilized ZrO_2 (YSZ), with 19 mm diameter and 2 mm thickness (Henson Ceramics Limited) was utilized as the solid electrolyte. Inert gold counter and reference electrodes were deposited on one side of the disk by applying thin gold paste coatings (Metalor, A1118) followed by calcination in air for 30 min at 450 °C and for 60 min at 650 °C. The Pd catalytic film was deposited on the other side of the solid electrolyte. The geometric surface area of the sputtered and impregnated Pd working electrode was 2 cm^2 for all samples of this study.

Sputtered samples were prepared using a magnetron sputtering system. High purity argon has been used as sputtering gas and the substrate temperature was kept stable during the deposition at 50 °C. The discharge characteristics have been controlled using a variable DC power supply (1 kV and 2 A). Pure Pd (99.95%) has been used as sputtering target. A thin Pd film was sputter-deposited on a YSZ disk with 167 target power, that enables 76 nm min^{-1} deposition rate and leads to a 380 nm film thickness after 5 min of deposition. During sputter-deposition the substrates were placed 55 cm far from the target which was found to result in good uniformity of the produced film. The final metal loading was measured by weighting the samples and was 0.8 ± 0.1 mg Pd for all sputtered samples.

Impregnated samples were prepared by successive steps of deposition and thermal decomposition of a Pd precursor solution [50]. An aqueous solution of 0.1 M $[Pd(NH_3)_4](NO_3)_2$ (Sigma–Aldrich) was used as the precursor. Initially, 20 μl of the precursor was applied on the YSZ substrate, using a plastic circular mask in order to obtain a 2 cm^2 geometric surface area of the catalytic film. Then, evaporation of the solvent took place

at 100 °C for 10 min, followed by drying the sample at 120 °C overnight and then calcination at 450 °C for 2 h. The procedure of successive steps of deposition, drying and heating was repeated until a final metal loading of 0.87 ± 0.01 mg Pd (total amount of 82 μl precursor solution) for all impregnated samples was obtained.

2.2. Catalyst characterization

The crystalline phases of the palladium catalysts and its support were examined by X-ray powder diffraction (XRD) performed in a PANalytical diffractometer equipped with a X'Celerator detector with monochromatic Cu Kα1 radiation (λ = 1.54 Å). XRD patterns were recorded in the 2θ range between 20° and 80°, with a scan step size of 0.017 and 610.5 s per step. Rietveld refinement of the data was performed using the Fullprof Suite program.

The X-ray photoelectron spectra were recorded on a K-Alpha (Thermo Scientific) spectrometer with a double-focusing hemispherical analyzer. The X-ray source provided monochromatic Al Kα radiation (1486.6 eV). Spectra were taken with a pass energy of 200 eV for survey spectra and 20 eV for high resolution spectra. The base pressure in the analysis chamber was 2×10^{-9} mbar. Sputtered and impregnated samples were placed on metal holders. The recording of the spectra as well as the data processing were carried out under identical conditions. The high resolution XPS spectra are presented without background subtraction. Peak area analysis was carried out on corrected spectra using a Shirley background subtraction.

The structure and morphology characterization of the different catalytic layers was carried out by Scanning Electron Microscopy (SEM) using a JEOL JSM-6300 microscope.

2.3. Reactor operation

Catalytic and electrocatalytic experiments were carried out in an atmospheric pressure single chamber quartz reactor with a volume of 30 cm^3, as described in detail elsewhere [39,42].

Reactants were Messer-Griesheim certified standards of 5.6% CH_4 in He, 10% C_2H_4 in He and 20% O_2. These mixtures could be further diluted in ultrapure (99.999%) He (L'Air Liquide). Gas flow rates were maintained using Brook mass flow controllers connected to a 4-channel Brose control box (model 5878). CH_4 and O_2 partial pressures were held constant at $P_{CH_4}/P_{O_2} = 2.6$ kPa/1.9 kPa, $P_{CH_4}/P_{O_2} = 1.4$ kPa/2.8 kPa, and $P_{CH_4}/P_{O_2} = 1.3$ kPa/4.5 kPa. The total flow rate in all the experiments was 170–200 $cm^3\,min^{-1}$ (STP).

Analysis of the reactants and products was performed using online gas-chromatography (Hewlett Packard 5890 Series II), while an infrared analyzer (Rosemount Binos 100) was used for the continuous and quantitative measurement of the CO_2 concentration. The gas chromatograph is equipped with a Thermal Conductivity Detector (TCD) and two columns, a Molecular Sieve 5A (for the separation of O_2, CH_4 and CO) and a Porapak Q column (for the separation of CH_4 and CO_2). TCD signals were integrated and recorded on line by the use of a Hewlett Packard integrator (model 3395).

During catalytic activity measurements, the in-plane resistance of the catalyst film was monitored. For this purpose the catalyst-electrode (working electrode) was connected to two point contacts (Au wires) placed at 8 mm distance from each other. The ohmic resistance between these two points was obtained with a Digital Multimeter (Mastech MY-68) during light off experiments and only under open circuit conditions. The application of constant currents or potentials was carried out using a SOLARTRON electrochemical interface 1286.

3. Results and discussion

3.1. Pre and Post experiment characterization of the Pd/YSZ catalyst-electrode

The difference in morphology and in phases of sputtered and impregnated Pd catalyst films has been investigated using SEM (Scanning Electron Microscopy), XRD (X-ray powder diffraction) and XPS (X-ray photoelectron spectroscopy). The choice of characterization methods was made as such to simultaneously obtain information with respect to the morphology of the palladium film (SEM), the crystalline structure and oxidation state of the catalyst (XRD), and the oxidation state of the external surface layer of the catalytic film (XPS). SEM pictures from the top view and cross section of the two different, as-prepared Pd/YSZ films are shown in Fig. 1. Both catalytic films exhibit similar morphology with equal porosity and roughness (Fig. 1a and c) and equal film thickness of ~2 μm (Fig. 2b and d). The Pd particles exhibit irregular distribution in size (2–50 μm) and shape which is mainly due to the surface roughness of the supporting disk. Both films show excellent adherence on the support and their porosity is sufficient to facilitate the migration of $O^{\delta-}$ promoter species from the solid electrolyte to the gas exposed surface of the catalytic film during NEMCA experiments [39,42].

The XRD patterns for the sputtered and impregnated samples are shown in Fig. 2. The crystal planes of the deposited films were identified according to the JCPDS crystallographic database [52].

Fresh sputtered samples show peak reflections of the metallic Pd form consistent with a face-centered cubic (fcc) structure where reflections appear at 40.1°, 46.6° and 68.1° corresponding to the (1 1 1), (2 0 0) and (2 2 0)planes of Pd^0 (JCPDS-ICDD Card No. 05-0681 [51]). After exposure to reaction conditions the Pd phase has been oxidized with peaks reflections appearing at 33.8°, 41.9°, 54.7° and 71.3° corresponding to the (1 0 1), (1 1 0), (1 1 2) and (2 0 2) planes of PdO (JCPDS-ICDD Card No. 41-1107 [51]). The presence of only metallic Pd for the fresh sputtered sample is expected since the film has been produced with a high purity palladium sputtering target in Ar environment without further treatment.

Fresh impregnated samples show peak reflections of PdO in consistence with a tetragonal structure where reflections appear at 33.8°, 41.9° and 54.7° corresponding to the (1 0 1), (1 1 0) and (1 1 2) planes of PdO (JCPDS-ICDD Card No. 41-1107 [51]). After EPOC experiments have been carried out at least part of the PdO is reduced to Pd^0 (Fig. 1b). The presence of only PdO in the fresh impregnated sample is due to the preparation process which includes a calcination step at temperature of 450 °C. PdO forms in presence of oxygen between 300 and 400 °C and is stable in air at atmospheric pressure up to 800 °C, depending on the support [1].

For both samples, the solid electrolyte shows the characteristic peaks of YSZ, $Zr_{0.8}Y_{0.2}O_{1.9}$, with peak reflections at 30.4°, 34.8°, 50.2°, 59.7°, 62.6° and 73.6° corresponding, to the (1 1 1), (2 0 0), (2 2 0), (3 1 1), (2 2 2) and (4 0 0) (JCPDS-ICDD Card No. 01-082-1246) [51]).

For sputtered samples, the crystallite size was calculated using the Debye–Scherrer equation. For the determination the experimental width of the Pd (1 1 1) and PdO (1 0 1) reflections are used in conjunction to Eq. (3):

$$D = \frac{0.9\vartheta_{Cu}}{\beta_{1/2}\ \cos\theta} \quad (3)$$

where ϑ_{Cu} is the X-ray wavelength, $\beta_{1/2}$ is the line broadening at half the maximum intensity (FWHM) in radians, and θ is the Bragg angle. The average crystallite size for the sputtered Pd sample is changing from 14 nm Pd^0 (fresh sample) to 18 nm for the PdO phase (after EPOC experiment). For the impregnated sample, the crystallite size has been obtained from Rietveld treatment of the XRD

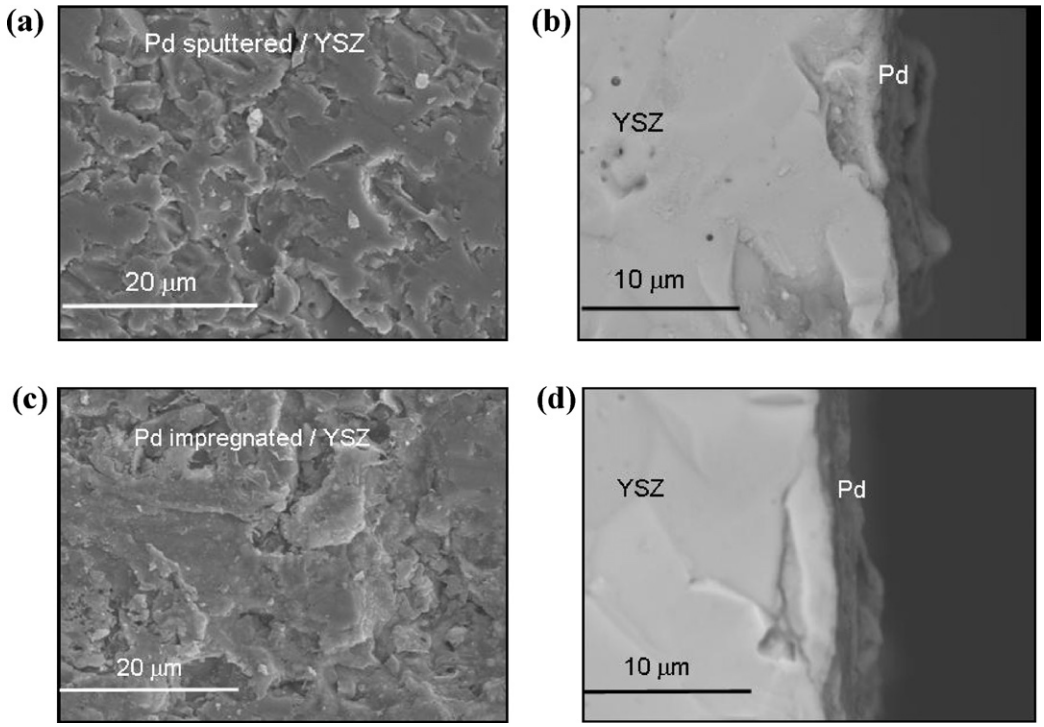

Fig. 1. SEM images for the catalyst-electrodes (a, b) Pd sputtered/YSZ and (c, d) Pd impregnated/YSZ before exposure to reaction conditions. The photographs in the left column show the top view of the samples, while the right column shows a cross section.

spectra. The crystallite size is changing from 14 nm of the PdO phase (fresh sample) to 29 nm for the Pd^0 phase (after EPOC experiment).

In the case of the sputtered sample, for the as prepared sample, the XPS spectrum in Fig. 3a shows a peak at lower binding energy value of Pd $3d_{5/2}$, 335.1 eV, which corresponds to the Pd metallic phase. This value is slightly higher than that reported for highly-dispersed metallic Pd, i.e. 334.5 eV [52]. This is most likely because the sputtered technique results in samples with lower dispersions than those prepared by impregnation or grafting. Moreover, there is a shoulder at a higher binding energy of 335.8 eV, which may indicate a slightly oxidized surface layer. Similar results were obtained by Neal et al. [53] for a PdO/p-TiO_2 catalyst after reduction in hydrogen at 170 °C. The surface oxidized layer may originate from the handling of the fresh sputtered sample in air, which can lead to the formation of PdO_x species on the metal particle surface. As for the used sputtered sample, both XRD and XPS results show that PdO is the only phase detected in this case.

For the fresh impregnated sample, the XPS analysis shows the Pd $3d_{5/2}$ peak at a binding energy of 337 eV (Fig. 3b), similar with the binding energies reported for PdO in the NIST database (335.6–337.1 eV) [52], which confirms the results observed by XRD, i.e. PdO is the only phase present in the fresh impregnated sample. However, for the impregnated used sample, there is an apparent disagreement between the XRD and XPS results. Bulk analysis (Fig. 2b – spent sample) shows no indication for the presence of cristalline PdO in this sample, while surface analysis (Fig. 3b) shows only peaks of PdO. This suggests that an oxidized surface is covering the metallic Pd particles formed on the electrolyte disk, and this layer is amorphous with a thickness larger than 5 nm, not allowing the detection of the oxide phase by XRD, nor of the metallic

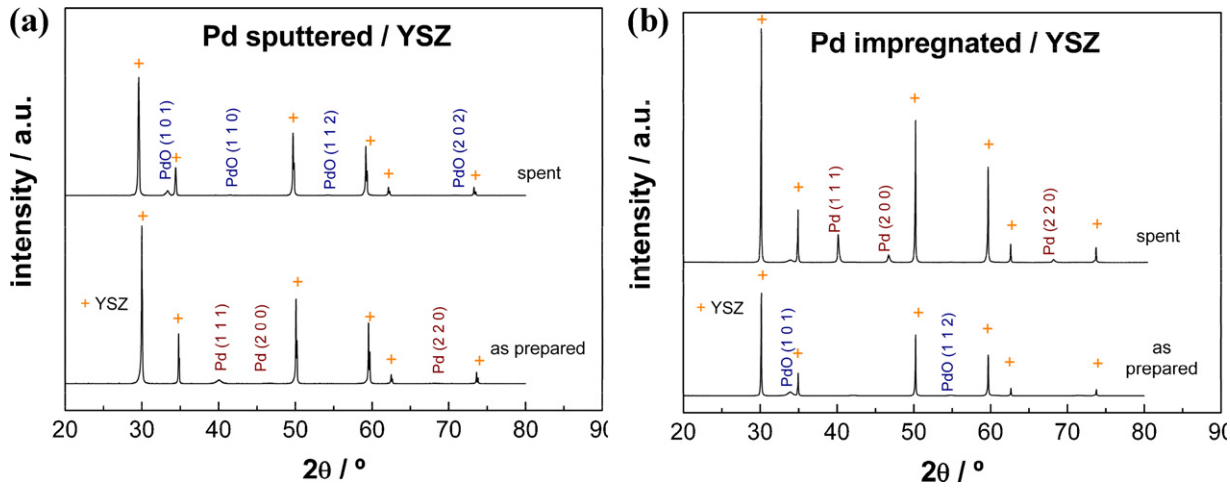

Fig. 2. XRD patterns for the catalyst-electrodes (a) Pd sputtered/YSZ and (b) Pd impregnated/YSZ before and after exposure to reaction conditions.

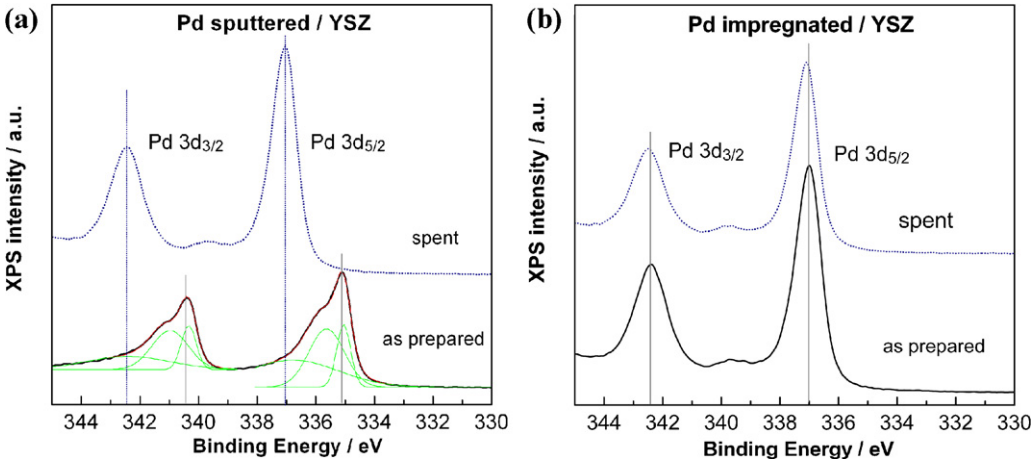

Fig. 3. High resolution Pd 3d XPS spectra for the catalyst-electrodes (a) Pd sputtered/YSZ and (b) Pd impregnated/YSZ before and after exposure to reaction conditions.

phase by XPS. Oxide layers covering a metallic Pd core have been previously proposed in the literature with similar behavior in XPS analysis [21,53].

The relatively low Pd loading for sputter-deposited and impregnated samples with 0.4 mg/cm^2, and the observed hysteresis loops of catalytic activity due to PdO/Pd reduction/oxidation cycles, which will be discussed in the next section, made it impossible to obtain reliable values for the free surface area of the electrode, or of its dispersion. The following techniques have been used, unsuccessfully, to investigate the Pd dispersion of spent catalysts: gas phase titration [39], in situ galvanostatic transient technique (EPOC experiment) [39,42] and chemisorption of H_2. In all cases, the free surface areas obtained experimentally were highly overvalued with 10^{-6} mol Pd/cm^2. This leads thus to an unlikely and overestimated high dispersion of almost 100%, and which is consistent with, at least partly, bulk oxidation of the Pd films. Additionally, as discussed in more detail in the next paragraph, significant activity hysteresis is observed for the Pd catalyst-electrodes, i.e. different methane combustion rates are found when the catalyst is either heated or cooled. This unusual kinetic behavior is discussed by a number of research groups [1,54–56] and is assigned to the decomposition of PdO to Pd and its re-formation.

3.2. Catalytic activity and the Pd–PdO phase transformation

Pd catalysts dispersed on YSZ exhibit excellent catalytic performance in ethylene oxidation with TOF approaching 50 s^{-1} [57], which led to the idea to pre-treat the sample in an oxidizing and reactive C_2H_4/O_2 mixture prior to methane oxidation. The co-feeding of small amounts of C_2H_4 to an overall oxidizing CH_4/O_2 reaction mixture, as well as reactive pre- treatment in an oxidizing C_2H_4/O_2 mixture led to enhanced methane combustion rates, as recently reported and discussed in detail by our group [50]. The second approach has been used successfully in the present study and comprises one thermal cycle with a ramp of 2 K min^{-1} from 120 to 450 °C and back to 120 °C in a mixture of $P_{C_2H_4} = 0.3$ kPa and $P_{O_2} = 4.5$ kPa. The pre-treatment led to significant enhancement of catalytic activity and even more important, electrochemically promoted methane oxidation was observed under fuel lean conditions at temperatures as low as 320 °C [50].

Since phase changes from PdO to Pd^0 and vice versa are expected to be accompanied by changes in conductivity, the catalytic activity measurements have been carried out with simultaneous in-plane resistance measurements and monitoring the open circuit potential.

Fig. 4 presents a comparison of sputtered and impregnated catalysts in terms of their catalytic activity for methane oxidation (top row), their in-plane resistance (middle row) and their open circuit potential as function of temperature before (1st run) and after treatment (2nd run) in an oxidizing and reactive C_2H_4/O_2 mixture. For sputtered catalyst-electrodes the original methane oxidation activity is very low over the entire temperature range, while impregnated Pd/YSZ catalysts exhibit already in the first run significant catalytic activity. Both catalysts show an improvement in methane conversion after pre-treatment. This treatment in a mixture of $P_{C_2H_4} = 0.3$ kPa and $P_{O_2} = 4.5$ kPa consists of a thermal cycling with a ramp of 2 K min^{-1} from 120 to 450 °C and back to 120 °C.

A significant activity hysteresis is observed for both catalyst-electrodes in the second run, i.e. different methane combustion rates are found when the catalyst is either heated or cooled. This hysteresis is observed in a more or less pronounced manner in the temperature dependence of the in-plane resistance (middle row) as well as of the open circuit potential (bottom row).

The as-prepared sputtered Pd film consists of Pd^0, which explains the very low catalytic activity and the near zero in-plane resistance observed in the heating branch of the 1st cycle. Its final resistance, marked with a circle after the first light-off, is close to 1.2 kΩ, the in-plane resistance of the as prepared impregnated sample, marked again with a circle in Fig. 4b. After treatment in an oxidizing ethylene-oxygen mixture, the methane light-off temperature drops to 200 °C and the conversion increases to 8% at 450 °C, while the resistance at 250 °C remains almost unchanged in comparison to the non-treated sample. The sputtered film shows the most significant changes in the in-plane resistance for the second light off experiment, which reflects that the oxidation of the Pd^0 film to PdO is activated. The changes in the in-plane resistance also reflect changes in the particle size in conjunction to the more general morphological changes of the catalyst.

For the as prepared impregnated sample, the in-plane resistance is slightly higher at the beginning of the experiment, due to the calcination step during preparation at 450 °C in air. It remains unchanged after treatment in C_2H_4/O_2, and in the second light off experiment. This provides evidence that PdO remains the major phase, though it becomes partially reduced to Pd^0, as suggested by the slight reduction of its in-plane resistance observed in Fig. 4b.

Results from the in-plane resistance measurements, i.e. the partial reduction of the PdO phase in case of the impregnated catalyst film (Fig. 4b) and the partial oxidation of the Pd metallic phase in the sputtered one (Fig. 4a), are confirmed by the changes observed in the open circuit potential (bottom row). Noble metal electrodes

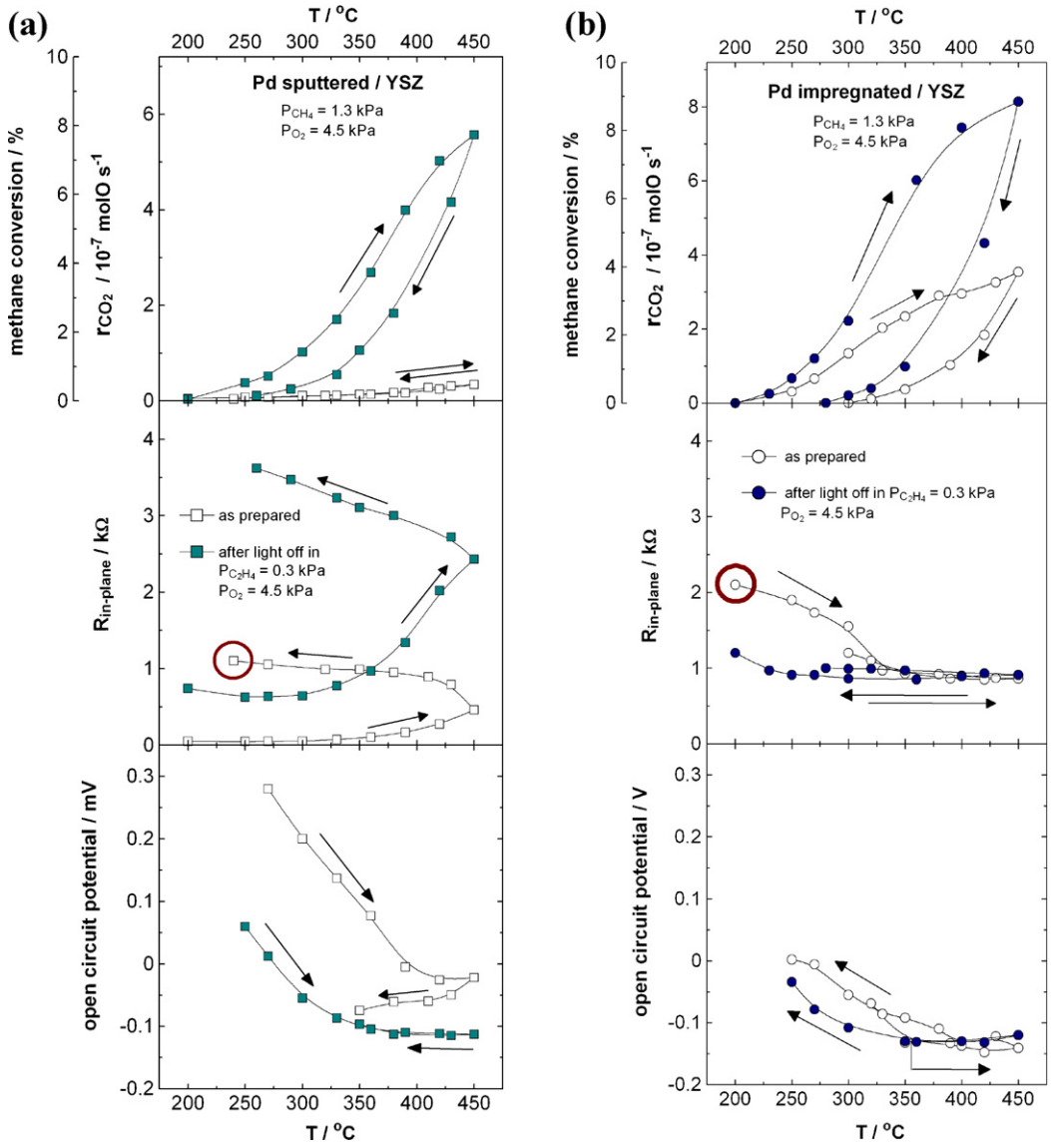

Fig. 4. Effect of temperature (top row) on methane conversion, (middle row) on in-plane resistance and (bottom row) on open circuit potential observed during light off. Column (a) represents results of the Pd sputtered/YSZ catalyst-electrode, column (b) those of the Pd impregnated/YSZ one. Open symbols represents results obtained for the as-prepared samples and closed symbols those after treatment. Reaction conditions: $P_{CH_4} = 1.3$ kPa, $P_{O_2} = 4.5$ kPa, treatment conditions: $P_{C_2H_4} = 0.3$ kPa, $P_{O_2} = 4.5$ kPa.

show generally high and positive open circuit potentials at temperatures below 300 °C, and potentials near zero, or slightly negative, at higher temperatures in overall oxidizing and reactive gas mixture [42]. Only the as prepared, non-treated, Pd sputtered film clearly shows this behavior.

Preliminary studies on pre-reduced impregnated samples have been carried out to study the influence of the Pd^0 phase on electropromotion ability. The impregnation and calcination steps for those catalysts were identical with the method used to obtain the impregnated samples in the present study. After preparation, the samples were reduced in 5% hydrogen, while heating to 550 °C and cooling to room temperature. The catalyst-electrodes exhibited near zero in-plane resistance and a shiny, reflective surface. They did not show any catalytic activity for methane combustion. Certainly, ethylene oxidation was possible at moderate temperatures. Electrochemical promotion experiments on such deeply reduced Pd films did not allow for changes in catalytic activity for temperatures of up to 450 °C. Obviously, the deep reduction of a Pd film deposited on YSZ hinders its re-oxidation [21,22].

3.3. Electrochemically promoted methane oxidation

The electrochemical promotion of methane oxidation on impregnated and sputtered Pd catalyst-electrodes has been studied in different methane/oxygen reaction mixtures and different temperatures. All results presented have been obtained on samples previously treated in an oxidizing C_2H_4/O_2 gas mixture in one thermal cycle from 120 to 450 °C and back.

Fig. 5a and 5b presents typical galvanostatic transient experiments for sputtered and impregnated Pd catalyst electrodes, respectively, carried out at 350 °C in oxidizing conditions and at constant positive current application of +1 mA. Fig. 5a shows, for example, that at $t < 0$ an open circuit catalytic rate, r_0, of 1×10^{-7} molO s^{-1} is observed for the sputtered sample. At $t = 0$, a positive current is applied and causes a slow increase in the CO_2 formation rate until a new value of $r = 1.6 \times 10^{-7}$ molO s^{-1} is reached. Due to the current application, oxygen ions, O^{2-}, are transferred from the YSZ support to the Pd catalyst-electrode at a rate of $I/2F$. The increase in the catalytic rate, Δr, of 0.6×10^{-7} molO s^{-1}, is 12

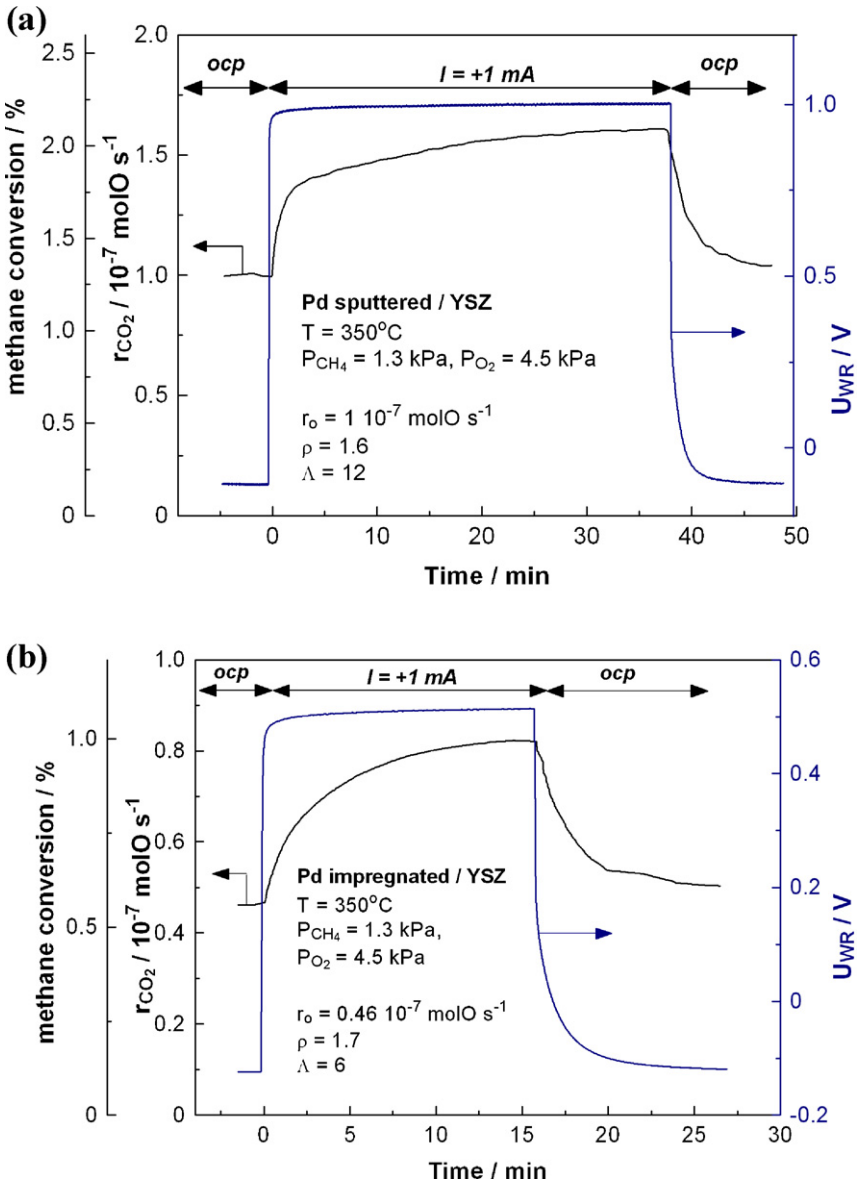

Fig. 5. Reaction rate of CO_2, methane conversion and catalyst potential response to a constant applied anodic current of I = 1 mA for (a) Pd sputtered/YSZ and (b) Pd impregnated/YSZ. Reaction conditions: T = 350 °C, P_{CH_4} = 1.3 kPa, P_{O_2} = 4.5 kPa.

times larger than the rate of ion transport, $I/2F$. This implies that each O^{2-} supplied to the Pd catalyst surface causes 12 chemisorbed O atoms to react with methane. The two parameters, the rate enhancement ratio and the Faradaic efficiency, have values of 1.6, and 12, respectively. After current interruption, the catalytic rate returns reversibly to its initial steady-state value.

Fig. 5b shows the transient effect of the application of +1 mA on the CO_2 formation rate for the impregnated sample. Similar with the sputtered one, the rate increases slowly with positive current application from an open-circuit value of 0.46×10^{-7} molO s^{-1} to 0.82×10^{-7} molO s^{-1}. The rate enhancement ratio is of the same order of magnitude with the sputtered sample, 1.7, and the Faradaic efficiency reaches 6. As in the case of the sputtered sample, after current interruption, the catalytic rate returns reversibly to its initial steady-state value.

Fig. 6 shows steady state electrochemical promotion results obtained for the methane oxidation on a sputtered film, prior and after treatment in C_2H_4/O_2. The Tafel plots, Fig. 6(top), show a decrease in the exchange current density for anodic polarization for the mostly metallic film from 0.2 mA/cm^2 to 0.08 mA/cm^2 for the treated electrode. Surprisingly, the non-treated sample exhibited a small increase in CO_2 formation rate at positive overpotentials with maximum ρ values of 2.6 and small Λ values of approximately 2, as seen in Fig. 6(bottom).

Fig. 6 shows clearly the advantages of electrochemical promotion, i.e. the current or potential induced increase in catalytic activity for an almost inactive catalyst, i.e. Pd^0 on YSZ. But it demonstrates on the other hand its limitations, when the low temperature catalytic active phase is an oxide (PdO) which can be obtained only after oxidative pretreatment of sputtered catalyst-electrodes. Impregnated Pd samples show higher open circuit catalytic activity, since after calcination the catalytic active PdO phase is formed. But the as prepared catalyst-electrodes could not be electropromoted over the entire temperature range investigated, mainly due to the total lack of metallic phase which seems to be one basic prerequisite for electrochemical promotion.

Fig. 7 shows Tafel plots, i.e. the current as a function of applied potential, U_{WR} for reducing, stoichiometric and oxidizing gaseous compositions at 350 °C comparing sputtered (Fig. 7a) and impregnated (Fig. 7b) catalyst-electrodes. For both samples the current

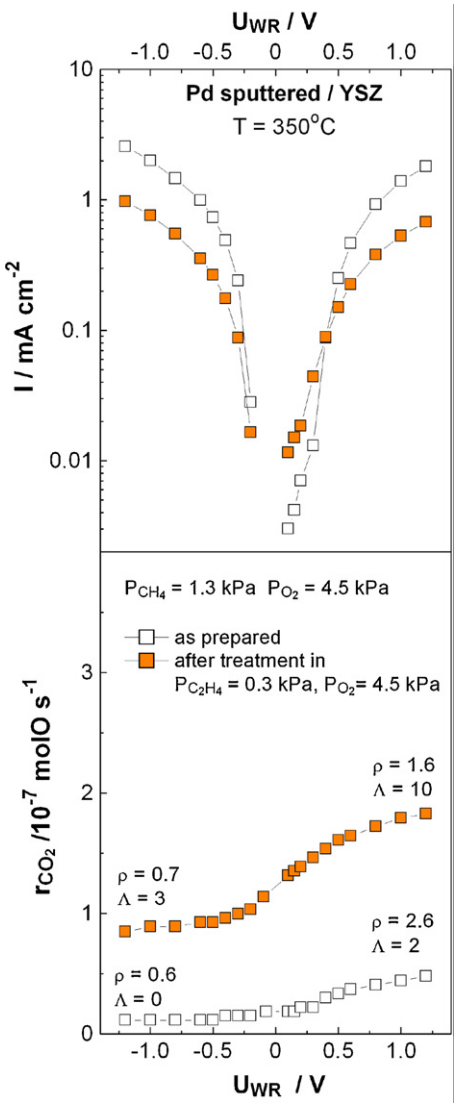

Fig. 6. Effect of applied potential on current (top) and on CO_2 formation (bottom) for a Pd sputtered/YSZ catalyst-electrode. Reaction conditions: $P_{CH_4} = 1.3$ kPa, $P_{O_2} = 4.5$ kPa, treatment conditions: $P_{C_2H_4} = 0.3$ kPa, $P_{O_2} = 4.5$ kPa.

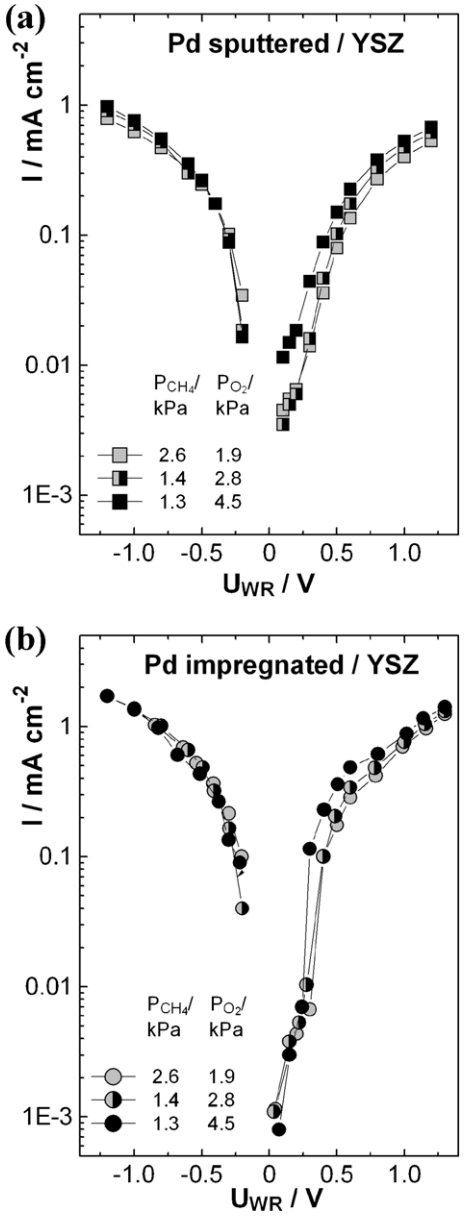

Fig. 7. TAFEL plots for three different gaseous compositions for (a) Pd sputtered/YSZ and (b) Pd impregnated/YSZ. Reaction conditions: $T = 350\,^{\circ}C$, open symbols: $P_{CH_4} = 2.6$ kPa, $P_{O_2} = 1.9$ kPa, semi-filled symbols: $P_{CH_4} = 1.4$ kPa, $P_{O_2} = 2.8$ kPa, filled symbols: $P_{CH_4} = 1.3$ kPa, $P_{O_2} = 4.5$ kPa.

exchange density is little affected by the gas composition and is of the order of 0.1–0.08 mA/cm^2. The CO_2 formation rate, not shown as a figure, increases at positive overpotentials and reaches maximum ρ values of 2.5, while cathodic polarization poisons methane oxidation. These findings are in agreement with previous kinetic studies on Pd paste [37] and Pd impregnated films which show near zero order kinetics with respect to the oxygen and first order in methane, both under open and closed circuit conditions.

Fig. 8 represents the effect of current on the induced catalytic rate change, Δr, expressed in molO s^{-1}. The absolute values of the Faradaic efficiency or enhancement factor, Λ, were typically 10–100 for the sputtered electrode and 2–10 for the impregnated ones. At low current, Λ values of up to 500 were measured. The order of magnitude of the measured enhancement factor, Λ, i.e. approximately 150 for sputtered catalyst-electrodes and near 10 for impregnated catalyst-electrodes, is in good qualitative agreement with the parameter $2Fr_0/I_0$, where r_0 is the open circuit (unpromoted rate) and I_0 is the exchange current density, as summarized in Table 2.

Fig. 9 shows a galvanostatic NEMCA transient with a sputtered Pd electrode, i.e. the response of the CO_2 formation rate for CH_4 oxidation and of the potential U_{WR} to the application of a current of -100 μA. As already discussed, electrophobic behavior is observed, i.e. the catalytic activity decreases under cathodic polarization. However, after current interruption, the CO_2 formation rate remains at a lower value than the initial steady state value at open circuit. This permanent poisoning phenomenon is observed at oxidizing, stoichiometric and reducing gas composition, but only for sputtered electrodes. Nakos et al. [45] observed a similar permanent poisoning behavior of methane oxidation on Rh/YSZ, i.e. the

Table 2
Electrokinetic parameters and open circuit catalytic rates ($P_{O_2} = 4.5$ kPa, $P_{CH_4} = 1.2$ kPa, $T = 350\,^{\circ}C$).

Catalyst	$I_{0,a}$ (mA)	r_0 (10^{-7} molO s^{-1})	$2Fr_0/I_0$	Λ_{exp}
Pd sputtered	0.1	1.14	220	~150
Pd impregnated	0.2	0.18	17	~10

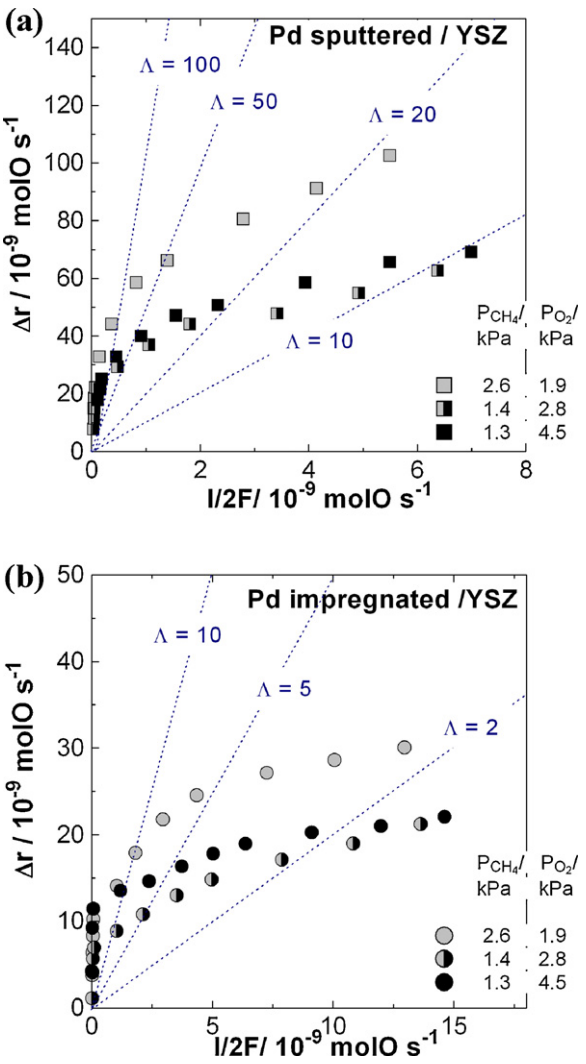

Fig. 8. Effect of the rate, $I/2F$, of electrochemical oxygen ion supply on the induced increase in the CO_2 formation rate, Δr, for three different gaseous compositions for (a) Pd sputtered/YSZ and (b) Pd impregnated/YSZ. Conditions as in Fig. 7.

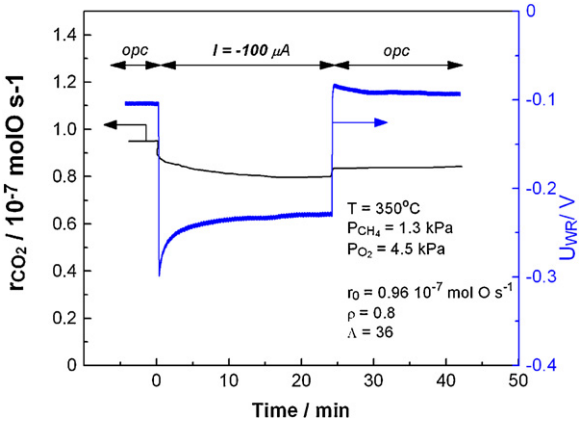

Fig. 9. Reaction rate of CO_2, methane conversion and catalyst potential response to a constant applied cathodic current for a sputtered Pd/YSZ. Reaction conditions: $T = 350\,^{\circ}C$, $P_{CH_4} = 1.4$ kPa, $P_{O_2} = 4.5$ kPa.

non-reversible change in catalytic activity, only under reducing conditions. They discuss their findings in view of the formation of a surface oxide layer due to stronger adsorption of gas phase oxygen under negative polarization. Hence a chemical potential gradient between catalyst surface and solid electrolyte support is developed, the thermal diffusion of O^{2-} is hindered after current interruption and catalytic activity remains therefore lower after returning to open circuit conditions [45]. In the case of Rh/YSZ as well as in the present case, under cathodic polarization chemisorbed oxygen is removed from the catalyst surface. As shown by XRD and XPS, the catalyst surface consists of PdO and cathodic polarization therefore can lead to the partial electrochemical reduction of surface Pd oxide accompanied with a decrease in catalytic activity. After current interruption, catalytic activity remains low due to the kinetically hindered Pd re-oxidation.

Nicole et al. [58] introduced the ratio γ, describing the fraction of the permanent modification of catalytic activity. Similar to this parameter, a rate poisoning index, β, can be defined in order to quantify the magnitude of the "poisoning permanent-EPOC" [45].

$$\beta = \frac{r_o - r_{poisoned}}{r_o} \quad (4)$$

where $r_{poisoned}$ is the catalytic rate in the "poisoned permanent-EPOC" steady-state after negative current application, and r_0 is the open-circuit catalytic rate. For reducing conditions, the poisoning index, β, is 0.10, indicating 10% lower catalytic activity after negative current application. Under stoichiometric conditions the poisoning index β is found to be 0.16, while for oxidizing conditions (Fig. 9), a value of 0.12 is obtained.

4. Conclusions

The effect of electrochemical promotion of catalysis (NEMCA effect or EPOC) was studied for the methane oxidation on Pd catalytic films interfaced with 8 mol% Y_2O_3-stabilized-ZrO_2 (YSZ), an O^{2-} conductor, under reducing, stoichiometric and oxidizing conditions, at a temperature range from 350 to 450 °C. The Pd films were deposited on the solid electrolyte using sputter-deposition, or the wet impregnation technique. The samples produced via both preparation techniques, exhibit electrophobic NEMCA behavior, i.e. the rate of CO_2 formation increases with positive current application, causing a 1.6-fold increase of the catalytic rate and a Faradaic efficiency of 12, for the sputtered sample, while for the impregnated sample a 1.7 rate enhancement rate is obtained, and the Faradaic efficiency reaches 6. After positive current interruption, the catalytic rate reversibly returned to the initial open-circuit values. However, negative current application led to a decrease of the rate, i.e. after negative current interruption the catalytic rate slowly increased, but remained in a lower than the initial value. This permanent poisoning phenomenon is observed under all used gas composition, but only for sputtered electrodes. Sputtered films consist primarily of the Pd metal phase and can be electropromoted without any pretreatment. Impregnated films need pretreatment in an oxidizing C_2H_4/O_2 mixture in order to exhibit electropromotion behavior.

Moreover, three different characterization methods were used to obtain information regarding the sputtered and impregnated samples. The XPS and XRD results give evidence for a PdO-Pd phase transformation in the analyzed samples. These results are also confirmed by the in-plane resistance measurements, which show partial reduction of PdO in the case of the impregnated sample and oxidation of Pd metallic for the sputtered sample, leading to the idea of an oxidized layer covering a metal core, consistent with previous literature reports.

Acknowledgments

Florina Matei gratefully thanks AM POS DRU of the Romanian Government for support through project POSDRU/88/1.5/S/56661. Carmen Jiménez-Borja gratefully thanks the Spanish Ministry of Science and Innovation for the FPI grant (BES-2008-002262) for her stay at the University of Patras.

References

[1] D. Ciuparu, M.R.L. Lyubovsky, E. Altman, L.D. Pfefferle, A. Datye, Catalysis Reviews 44 (2002) 593–649.
[2] P. Forzatti, Catalysis Today 83 (2003) 3–18.
[3] P. Gélin, M. Primet, Applied Catalysis B: Environmental 39 (2007) 1–37.
[4] G. Centi, Journal of Molecular Catalysis A: Chemical 173 (2001) 287–312.
[5] Y.H. Chin, D.E. Resasco, Catalysis 14 (1999) 1–39.
[6] R. Burch, F.J. Urbino, Applied Catalysis A: General 124 (1995) 121–138.
[7] A.K. Datye, J. Bravo, T.R. Nelson, P. Atanasove, M. Lyubovsky, L. Pfefferle, Applied Catalysis A: General 198 (2000) 179–196.
[8] N.M. Kinnunen, J.T. Hirvi, T. Venäläinen, M. Suvanto, T.A. Pakkanen, Applied Catalysis A: General 397 (2011) 54–61.
[9] M. Lyubovsky, Lisa Pfefferle, Applied Catalysis A: General (1998) 107–119.
[10] G.W. Graham, D. Koenig, B.D. Poindexter, J.T. Remillard, W.H. Weber, Topics in Catalysis 8 (1999) 35–45.
[11] D. Koenig, W.H. Weber, B.D. Poindexter, J.R. McBride, G.W. Graham, K. Otto, Catalysis Letters 29 (1994) 329–338.
[12] G.B. Hoflund, H.A.E. Hagelin, J.F. Weaver, G.N. Salaita, Applied Surface Science 205 (2003) 102–112.
[13] R.J. Farrauto, J.K. Lampert, M.C. Hobson, E.M. Waterman, Applied Catalysis B: Environmental B6 (1995) 263–270.
[14] N. van Vegten, M. Maciejewski, F. Krumeich, A. Baiker, Applied Catalysis B: Environmental 93 (2009) 38–49.
[15] S. Yang, A. Maroto-Valiente, M. Benito-Gonzales, I. Rodriguez-Ramos, A. Guerrero-Ruiz, Applied Catalysis B: Environmental 28 (2000) 223–233.
[16] M. Schmal, M.M.V.M. Souza, V.V. Alegre, M.A. Pereira da Silva, D.V. César, C.A.C. Perez, Catalysis Today 118 (2006) 392–401.
[17] K. Sekizawa, H. Widjaja, S. Maeda, Y. Ozawa, K. Eguchi, Catalysis Today 59 (2000) 69–74.
[18] C.A. Müller, M. Maciejewski, F. Krumeich, A. Baiker, Catalysis Today 47 (1999) 38–49.
[19] D. Ciuparu, E. Altman, L. Pfefferle, Journal of Catalysis 203 (2001) 64–74.
[20] D. Ciuparu, L.D. Pfefferle, Applied Catalysis A: General 218 (2001) 197–209.
[21] S.C. Su, J.N. Carstens, A.T. Bell, Journal of Catalysis 176 (1998) 125–135.
[22] F. Arosio, S. Colussi, A. Trovarelli, G. Groppi, Applied Catalysis B: Environmental 80 (2008) 335–342.
[23] D.E. Williams, Sensors and Actuators B: Chemical 57 (1–3) (1999) 1–16.
[24] N. Barsan, D. Koziej, U. Weimar, Sensors and Actuators B: Chemical 121 (1) (2007) 18–35.
[25] T. Hübert, L. Boon-Brett, G. Black, U. Banach, Sensors and Actuators B: Chemical 157 (2) (2011) 329–352.
[26] B.K. Lai, K. Kerman, S. Ramanathan, Journal of Power Sources 196 (2011) 6299–6304.
[27] F. Liang, W. Zhou, B. Vhi, J. Pu, S.P. Jiang, L. Jian, International Journal of Hydrogen Energy 36 (2011) 2040–2051.
[28] Md. Ariful Hoque, S. Lee, N.-K. Park, K. Kim, Catalysis Today 185 (2012) 66–72.
[29] J. Mizsei, P. Sipilä, V. Lantto, Sensors and Actuators B: Chemical 47 (1998) 139–144.
[30] H.J. de Bruin, S.P.S. Badwal, Journal of Solid State Chemistry 34 (1980) 133–135.
[31] S.P.S. Badwal, Journal of the Electrochemical Society 129 (1982) 1921.
[32] H. Kaneko, A. Nagai, H. Taimatsu, Solid State Ionics 35 (1989) 257–262.
[33] K. Kalimeri, G. Pekridis, S. Vartzoka, C. Athanassiou, G. Marnellos, Solid State Ionics 177 (2006) 979–988.
[34] K. Yokari, S. Bebelis, Journal of Applied Electrochemistry 30 (2000) 1277–1283.
[35] S. Seimanides, M. Stoukides, Journal of Catalysis 98 (1986) 540–549.
[36] A. Giannikos, A.D. Frantzis, C. Pliangos, S. Bebelis, C.G. Vayenas, Ionics 4 (1998) 53–60.
[37] A.D. Frantzis, S. Bebelis, C.G. Vayenas, Solid State Ionics 136–137 (2000) 863–872.
[38] C.G. Vayenas, S. Bebelis, S. Ladas, Nature 343 (1990) 625–628.
[39] C.G. Vayenas, S. Bebelis, C. Pliangos, S. Brosda, D. Tsiplakidis, Electrochemical Activation of Catalysis: Promotion, Electrochemical Promotion and Metal–Support Interactions, Kluwer Academic/Plenum Publishers, NY, 2001.
[40] G. Foti, I. Bolzonella, Ch. Comninellis, in: C.G. Vayenas, B.E. Conway, R.E. White (Eds.), Electrochemical Promotion of Catalysis, Modern Aspects of Electrochemistry, no. 36, Kluwer Academic/Plenum Publishers, New York, 2003, pp. 191–254.
[41] C. Jiménez-Borja, A. de Lucas-Consuegra, J.L. Valverde, F. Dorado, Á. Caravaca, J. Gonzáles, in: J.C. Taylor (Ed.), Advances in Chemical Research, vol. 14, Nova Science Publishers, Inc., 2012 (Chapter 4), in press.
[42] C.G. Vayenas, C.G. Koutsodontis, Journal of Chemical Physics 128 (2008) 182506-1–182506-13.
[43] P. Tsiakaras, C.G. Vayenas, Journal of Catalysis 140 (1993) 53–70.
[44] E.A. Baranova, G. Fóti, Ch. Comninellis, Electrochemistry Communications 6 (2004) 170–175.
[45] A. Nakos, S. Souentie, A. Katsaounis, Applied Catalysis B: Environmental 101 (2010) 31–37.
[46] V. Roche, R. Karoum, A. Billard, R. Revel, P. Vernoux, Journal of Applied Electrochemistry 38 (2008) 1111–1119.
[47] V. Roche, R. Revel, P. Vernoux, Catalysis Communications 11 (2010) 1076–1080.
[48] C. Jiménez-Borja, F. Dorado, A. de Lucas-Consuegra, J.M. García-Vargas, J.L. Valverde, Catalysis Today 146 (2009) 326–329.
[49] C. Jiménez-Borja, S. Brosda, M. Makri, F. Sapountzi, F. Dorado, J.L. Valverde, C.G. Vayenas, Solid State Ionics (2012), http://dx.doi.org/10.1016/j.ssi.2012.03.004, in press.
[50] C. Jiménez-Borja, S. Brosda, F. Matei, M. Makri, B. Delgado, F. Sapountzi, D. Ciuparu, F. Dorado, J.L. Valverde, C.G. Vayenas, Applied Catalysis B: Environmental (2012), http://dx.doi.org/10.1016/j.apcatb.2012.02.011, in press.
[51] JCPDS-ICD, PCPDFWIN, Version 2.2 June 2001.
[52] National Institute of Standards and Technology, NIST On-Line XPS Database, http://srdata.nist.gov/xps/intro.aspx.
[53] L. Neal, M. Everett, G. Hoflund, H. Hagelin-Weaver, Journal of Molecular Catalysis A: Chemical 335 (2011) 210–221.
[54] H. Gabasch, K. Hayek, B. Klötzer, W. Unterberger, E. Kleimenov, D. Teschner, S. Zafeiratos, M. Hävecker, A. Knop-Gericke, R. Schlögl, B. Aszalos-Kiss, D. Zemlyanov, Journal of Physical Chemistry C111 (2007) 7957–7962.
[55] R.S. Monteiro, D. Zemlyanov, J.M. Sorey, F.H. Ribeiro, Journal of Catalysis 201 (2001) 34–45.
[56] J. Han, D. Zemlyanov, F.H. Ribeiro, Catalysis Today 117 (2006) 506–513.
[57] C. Pliangos, I.V. Yentekakis, V.G. Papdakis, C.G. Vayenas, X.E. Verykios, Applied Catalysis B: Environmental 14 (1997) 161–173.
[58] J. Nicole, D. Tsiplakides, S. Wodiunig, Ch Comninellis, Journal of the Electrochemical Society 144 (1997) L312–L314.